Geoderma 473 (2026) 117995

Contents lists available at ScienceDirect

Geoderma

journal homepage: www.elsevier.com/locate/geoderma

Soil structure evolution after gypsum, structure lime and pulp mill sludge applications: The amendment type matters

Jari Hyväluoma [a,*], Idil Ertem [b,c], Arttu Miettinen [c], Janne Kaseva [a], Helena Soinne [d], Sami Kinnunen [c], Tero Harjupatana [c], Riikka Keskinen [a]

[a] Natural Resources Institute Finland (Luke), Tietotie 4, FI-31600 Jokioinen, Finland
[b] Natural Resources Institute Finland (Luke), Survontie 9 A, FI-40500 Jyväskylä, Finland
[c] Department of Physics, University of Jyväskylä, Survontie 9 C, PO BOX 35, FI-40014 Jyväskylä, Finland
[d] Natural Resources Institute Finland (Luke), Latokartanonkaari 9, FI-00790 Helsinki, Finland

ARTICLE INFO

Handling Editor: Yvan Capowiez

Keywords:
Soil structure
Soil amendment
Macropores
X-ray tomography
Image analysis

ABSTRACT

Various soil amendments are used to improve soil structural stability against water erosion. Gypsum, structure lime and pulp mill sludges have all received interest in northern conditions and shown positive results in this respect. However, only a few studies have focused on the impacts of amendments on soil pore systems, particularly on their temporal dynamics under field conditions. In this study, we used X-ray tomography for time-lapse imaging of field-incubated soil samples to follow the structural dynamics of clay soil treated with gypsum, structure lime, or pulp mill sludge. Our results showed that gypsum and structure lime did not notably influence the macropore structure dynamics as compared to the non-treated control. In contrast, pulp mill sludge altered the macropore system significantly in comparison to control and two inorganic amendments. Pulp mill sludge increased the share of large macropores (>1200 μm), whereas the smaller macroporosity (<300 μm) temporarily decreased after the initiation of field incubation. After the first winter, the differences in this pore size region between the treatments levelled off. Our results show that, in addition to soil structural stability, soil amendments can influence the soil macropore system, but the magnitude and nature of these effects strongly depend on amendment type.

1. Introduction

Soil improvement has a long history, and a wide variety of soil amendments has been used for improving the properties of arable soils (Garbowski et al. 2023). Examples of organic soil amendments include livestock manures, plant residues, slaughterhouse wastes, sewage sludge and algae, which can be used as such or further processed by composting, anaerobic digestion or pyrolysis (Barthod et al. 2018; O'Connor et al. 2022; Keskinen et al. 2020). Inorganic substances have also been used for soil improvement including, e.g., lime, gypsum and clay minerals (Holland et al. 2018; Kost et al. 2018; Tahir & Marschner 2016). Soil amendment aims at enhancing the soil productivity and crop yields, or reducing the environmental impacts of agricultural production, such as nutrient and sediment loading to water bodies. Possible impacts of soil amendments include enhanced supply and availability of nutrients for plant growth, enhanced or maintained biological activity, improved stability of soil aggregates and changes induced to the soil pore networks (Larney & Angers 2012).

Of the large variety of soil amendments, three substances are currently of major interest among Finnish decision makers and farmers, namely gypsum, structure lime and sludges originating from pulp and paper industry, due to their effectiveness as water protection measures through soil structure stabilization (Keskinen et al. 2025). In this region, gypsum ($CaSO_4 \cdot 2H_2O$) is available in large quantities as a byproduct of phosphoric acid production for fertilizer manufacture (Iho & Laukkanen 2012). Gypsum application introduces additional Ca^{2+} ions into the soil solution, which increases the ionic strength and favours flocculation of negatively charged clay colloids (Uusitalo et al. 2012). Structure lime is composed of quicklime (CaO) or slaked lime ($Ca(OH)_2$) mixed with ground limestone ($CaCO_3$), where the fraction of the former highly reactive part typically comprises approximately 20 % of the liming product (Blomquist et al. 2023). Structure lime is to a limited extent available as recycled material. It can also be manufactured from pristine materials, which is, however, not environmentally feasible due to high

* Corresponding author.
E-mail address: jari.hyvaluoma@luke.fi (J. Hyväluoma).

https://doi.org/10.1016/j.geoderma.2026.117995
Received 28 May 2026; Received in revised form 16 July 2026; Accepted 14 August 2026
Available online 17 August 2026

climate impact (Ollikainen et al. 2024). Structure lime induces clay colloid flocculation and aggregation of soil by increasing the ionic strength of the soil solution similarly to gypsum. If used at high rates, structure lime can result in pozzolanic cementation reactions, which require a highly alkaline soil environment (pH≈12.4) (Al-Mukhtar et al. 2010). These reactions are exploited in stabilizing soils in civil engineering (Tan et al. 2020), but the required pH level is not reached with typical application rates used in agricultural applications (Soinne et al. 2025). Liming can also affect soil conditions through pH increase, which drives many chemical processes and may stimulate root growth and activity of soil biota (Holland et al. 2018). Pulp mill sludges are side streams from the wastewater treatment processes of the pulp and paper industry (Camberato et al. 2006). As organic materials, they affect soil structure in differing mechanisms as compared to gypsum and structure lime. When mixed with soil, these sludges enhance microbial activity, and the decomposition produces organic substances that stabilize the soil structure (Rasa et al. 2021). The added fibre material has been found to decompose relatively fast in a time scale of a few years (Foley & Cooperband 2002; Rasa et al. 2021). Nevertheless, part of the added material can remain in soil for decades (Heikkinen et al. 2021).

Most of the previous research on these soil amendments has focused on possibilities to reduce soil erosion and thus reduce phosphorus loading from agricultural fields to watercourses (Uusitalo et al. 2012; Ekholm et al. 2024; Ulén and Etana, 2014; Blomquist et al. 2022a; Rasa et al. 2021). However, little is known about their effects on soil architecture (i.e., the three-dimensional spatial arrangement of solid matter and pore spaces in soil across different scales), even though they are often claimed to improve both soil structure and its stability. Lime application may increase the soil macroporosity due to changes in soil chemistry and the abundance of earthworms and enchytraeids (Grieve et al. 2005). However, there are many studies that do not report changes in soil physical conditions due to liming, whereby the response of soil structure to liming is not clear (Holland et al. 2018). Regarding the structure liming, Bölscher et al. (2021) investigated the changes in the soil pore system at structure lime-treated fields in Sweden. They reported that structure liming decreased the soil macroporosity and shifted the pore size distribution from larger (>300 μm) macropores towards smaller pore sizes. The changes were reported to be site-specific, whereby the generalizability of the results is unclear (Bölscher et al. 2021). An earlier Swedish study focusing on structure liming found no effect on soil macroporosity (Hellner et al. 2018). Rasa et al. (2024) investigated the impacts of pulp mill sludges on the soil pore structure in a Finnish clay field where a large single addition of three different organic sludges had been applied. Sludge application had a significant impact only on macroporosity (>80 μm). However, no effect on intra-aggregate porosity was observed, even though significant improvement of soil structural stability had been observed in the same field earlier (Rasa et al. 2021).

Soils are known to be spatially heterogeneous such that soil properties, including structural attributes, may notably vary even at distances shorter than 1 m (Koszinski et al. 1995; Poeplau et al. 2022). This heterogeneity often complicates or prevents finding statistically significant differences at the plot scale, as the possible treatment-induced effects are hidden by the natural variation. One option to overcome this hardship could be to use a ‘semi-field’ approach to follow the structural dynamics of differently treated confined samples exposed to natural field conditions. X-ray tomography, as a non-destructive three-dimensional imaging method, enables repeated time-lapse tracking of pore network properties of samples that are field incubated in natural soil and weather conditions between scans. Such an approach has been used in a few soil studies. Koestel and Schlüter (2019) demonstrated the potential of the approach by following the structural evolution of a single soil sample installed in a field soil. Leuther et al. (2023) included structure labelling with inert garnet particles in the setup to quantify the structure turnover time of soil. Arrázola Vásquez (2023) monitored earthworm burrow systems using repeated X-ray tomography imaging and studied burrowing and casting rates over time. However, to the best of our knowledge, such an approach has not been used to study the impacts of soil amendments on soil structure. Obviously, while the approach utilizing time-lapse imaging enables investigation of soil structure-forming processes in field conditions, the excavation and re-installation of samples affect the interaction between the sample and surrounding soil, e.g., by breaking the roots that have entered the sample.

X-ray tomography provides direct information about the soil macropore structure. The soil macropore system can be segmented from three-dimensional images and analysed for structural characteristics such as porosity and pore-size distribution. In addition to structural properties, the imaged macropore network can be used as a simulation geometry for pore-scale numerical flow simulations, thereby providing information about the impacts of soil structure on the hydraulic functioning of soil (Hyväluoma et al. 2018; Schlüter et al., 2020). One appropriate approach for such simulations is the lattice Boltzmann method, which has proven to be suitable for simulating flow in porous media at the pore scale (Liu et al. 2016).In the present work, we aimed to investigate the effects of the three above-described soil amendments on the dynamics of soil structure in a clay soil. The samples were exposed to natural field conditions in a boreal climate and followed for one year. We used time-lapse imaging of field-incubated samples, which allowed the samples to experience natural environmental conditions while simultaneously reducing the confounding effects of spatial heterogeneity in soil structural properties. The applied imaging approach with a voxel size of 37.4 μm limited the study to soil macroporosity. Both image analysis and pore-scale flow simulations were used to quantify the impacts of the amendments on the structural characteristics and hydraulic functioning of the soil macropore system. Our research question was whether the studied soil amendments influence soil structure evolution relative to non-amended soils, and whether the structural responses differ among amendment types.

2. Materials and methods

2.1. Experimental setup

The soil used in the experiment was collected from an arable field located in the Savijoki catchment in Lieto, southwest Finland (60.58°N, 22.67°E). The soil was a silty clay loam classified as Vertic Luvic Stagnosol according to the WRB system (Lilja et al., 2017). The mineral fraction had a particle size distribution with 38 % clay (particle size < 0.002 mm), 32 % silt (0.002–0.02 mm), 29 % fine sand (0.02–0.2 mm) and 1 % sand (0.2–2 mm). The organic carbon content of the soil was 2.4 %, whereby the clay-to-carbon ratio was 16. The soil pH was 6.0. Before sample preparation, the soil was sieved through a 15 mm mesh.

Three soil amendments were considered in the study, i.e. gypsum, structure lime and lime-stabilized pulp mill sludge. All the materials were commercially available industrial by-products and were applied as supplied by the manufacturers. Gypsum originated from phosphoric acid production, where apatite is treated with sulfuric acid (Yara). Structure lime and pulp mill sludge are by-products from causticizing and wastewater treatment in pulp production, respectively. These products were productized and retailed by Soilfood Ltd. The pulp mill sludge used had been hygienised by lime stabilization (pH at the time of sample preparation was 10.9). The dry matter contents were 81 % for gypsum, 76 % for structure lime and 31 % for pulp mill sludge. Total carbon contents were 34 % for pulp mill sludge and 4.3 % for structure lime. The carbon content of gypsum was assumed negligible. The amendments were thoroughly mixed to the soil using the commonly used application rates in Finland for field use, i.e., 4000, 2700 and 30000 kg ha^{-1} for gypsum, structure lime, and pulp mill sludge, respectively, scaled to the surface area of the sample cylinders.

The soil was packed into PVC cylinders with an inner diameter of 46 mm and a height of 70 mm. The cylinders were perforated with 72 holes drilled using a 2.5 mm drill bit. The bottom of each cylinder was covered with frost cloth and nylon netting with a 1.5 mm mesh size. The same netting was used to cover the top of the cylinder after packing the cylinder with soil. The purpose of the selected hole and mesh sizes was to prevent the access of burrowing macrofauna tothe cylinders but to allow movement of smaller biota as well as water and solutes between the samples and the surrounding soil. Cylinders were packed with 120 g soil as dry mass at 83 % dry matter content to a bulk density of 1.1 g cm^{-3}. The sample preparation aimed at samples representing topsoil after seedbed preparation. The four treatments were soil amended with gypsum (G), structure lime (SL), pulp mill sludge (PMS), and unamended control (CTRL). In total, 16 samples were prepared with four replicate samples for each treatment.

The samples were placed in a field located in Laukaa, Central Finland (62.32°N, 26.11°E) to minimize time out of field during subsequent transportations and imaging. The samples were imaged with X-ray tomography (see next section) before placing them in the soil. Each sample cylinder was installed in a separate small soil pit, where the sample was surrounded with the same amended soil that was used to fill that cylinder. The sample was also covered with the same amended soil. The sample positions were randomized in a Latin square design, with row and column representing the two blocking factors. During the field incubation, the samples were removed from the field three times for X-ray tomography scanning. After each imaging, the samples were re-installed in the soil. Between the scans, samples were exposed to the field conditions and natural temperature and moisture fluctuations in the soil.

The field incubation began on June 18, 2024, when the initial imaging of the packed samples was conducted (hereinafter referred to as imaging round 0), and the samples were installed for the first time. Following imaging was performed on August 20–21, 2024 (round 1), and the next one on October 2–3, 2024 (round 2). The final imaging was done after the winter on May 13–14, 2025 (round 3). Thus, the entire study period lasted approximately one year.

The field incubation site is located in the boreal climate zone. According to the data from the closest weather station of the Finnish Meteorological Institute located ca. 20 km northwest of the site, the minimum and maximum temperatures during the incubation period were −24 °C (January 5, 2025) and 29 °C (June 28, 2024), respectively. The total rainfall during the period was 485 mm, and the maximum rainfall intensity was 21.7 mm h^{-1} (September 14, 2024). The maximum snow depth was 37 cm (March 16, 2025).

2.2. X-ray tomography and image analysis

The soil samples were scanned using an in-house built JTomo X-ray computed microtomography system at the University of Jyväskylä (X-ray Tomography Laboratory). The setup combines a Hamamatsu L12161-07 X-ray tube (40–150 kV, 75 W) with a Teledyne Shad-o-Box 6 K HS flat-panel detector arranged in a cone-beam configuration. Scans were performed at a tube voltage of 150 kV and a tube current of 150 μA under continuous rotation. For each sample, a full 360° rotation was acquired using 2940 projections with an exposure time of 250 ms per projection, and the reconstructed images were scaled to an isotropic voxel size of 37.4 μm to reduce noise. Three-dimensional volumes were reconstructed using a cone-beam Filtered Backprojection approach based on the Feldkamp–Davis–Kress algorithm (Feldkamp et al., 1984).

The greyscale images obtained from the X-ray tomography were converted to binary form. First, greyscale values of the images were calibrated using the greyscale values for the cylinder wall and air as reference densities and converted to 8-bit form (cf Larsbo et al. 2014; Turunen et al. 2019). The greyscale images were denoised with a three-dimensional variance-weighted mean filter with a radius of 2 voxels (Gonzalez and Woods 2008). Thereafter, the images were segmented into solid and pore phases by manual thresholding. The threshold greyscale value was selected to give the best segmentation of pores and solids as compared to visual inspection, and the same threshold value was applied for all images. The segmented image was further filtered by removing small isolated solid objects from the solid phase. The use of calibrated greyscale values and a single threshold value for all images avoided operator-induced bias in the segmentation. The top and bottom parts of the sample and the volume in the vicinity of the cylinder walls were excluded from the image analyses to prevent packing-induced perturbations and boundary effects in the image analysis results.

Segmented macropores were analysed for porosity and pore size distribution. The total macroporosity visible in the images was calculated from the segmented binary image by dividing the total number of pore voxels by the total number of voxels in the region of interest. Pore size distribution was calculated by successive application of a morphological opening operation (Horgan, 1998) with increasing diameter of the structuring element. Here, the pore space was divided into six pore size classes, i.e., <150 μm, 150–300 μm, 300–600 μm, 600–1200 μm, 1200–2000 μm and > 2000 μm, where the pore size refers to the pore diameter determined by the size of the structuring element. Note that the porosity results presented contain only that porosity larger than the imaging resolution, and the pore size class < 150 μm also contains only that porosity visible within the imaging resolution.

2.3. Flow simulations

Water flow through the imaged macropore system was simulated with the lattice Boltzmann method (e.g., Liu et al. 2016). The pore-scale steady-state flow field for saturated pressure-driven flow was simulated. The lattice Boltzmann method used operates on a uniform cubic lattice, and the segmented images obtained with X-ray tomography were directly used as the computational grid to describe the pore geometry of the samples. The D3Q19 lattice Boltzmann model with the two-relaxation-time collision operator was used (Ginzburg et al. 2008), where the even and odd relaxation times were related by the so-called "magic formula" (d'Humiéres & Ginzburg, 2009). The bounce-back boundary condition was used to enforce no-slip flow at the pore walls. The hydraulic conductivity (K_{sat}) of the sample was determined from the simulated flow field using the Darcy law. Further details of the used implementation can be found, e.g., in Hyväluoma et al. (2018).

2.4. Statistical analyses

Pore size distribution data derived from X-ray tomography were analysed using linear mixed models (LMM) to account for the hierarchical and repeated-measures structure of the experiment. The response variable was the porosity of individual pore size classes (<150 μm, 150–300 μm, 300–600 μm, 600–1200 μm, 1200–2000 μm and > 2000 μm). Porosity values were log-transformed prior to analysis to improve normality and homoscedasticity, and model estimates were presented on the original scale using the inverse link function. The fixed-effects structure included treatment (CTRL, G, SL, PMS), pore size class, imaging round (four time points), and all their interactions. Least-squares means and their corresponding 95 % confidence intervals were estimated for main effects and interactions.

Random effects were specified to account for the experimental layout and repeated measurements. Spatial variation was modelled by including row, column, and their interactions with imaging round as random effects. Temporal correlation arising from repeated imaging of the same cylinders was modelled using a compound symmetry (CS) covariance structure for imaging round within each cylinder × treatment combination (G-side). Variability among pore size classes within each imaging round and cylinder × treatment unit was modelled using an unstructured residual covariance matrix (R-side). An unstructured covariance matrix imposes no assumptions on the pattern of covariances, whereas CS assumes a constant covariance between all imaging rounds. The lowest Akaike information criterion (AIC) value was used as the primary criterion for covariance structure selection, together with evaluation of residual normality.

Degrees of freedom were calculated using the Kenward–Roger method to provide accurate inference under the complex covariance structure. Pairwise comparisons among treatments, pore size classes, and imaging rounds were performed using Tukey-adjusted tests. Planned comparisons derived from the three-way interaction were evaluated using sliced tests, fixing two of the factors; for example, treatment effects were compared separately within each pore size class and imaging round. Similarly, imaging rounds were compared within each pore size class and treatment. Statistical significance was assessed at $\alpha = 0.05$.

Total porosity and K_{sat} were analysed using analogous mixed-model structures without the pore size class factor. Because K_{sat} was strongly right-skewed, it was log-transformed prior to analysis to improve normality and homoscedasticity. For K_{sat}, unequal residual variances were allowed among treatments to account for heterogeneity of varianceThe random-effects structure was otherwise similar to that used for pore size distribution. Temporal correlation between repeated imaging rounds was accounted for on the R-side, using a compound symmetry (CS) covariance structure for total porosity and a heterogeneous autoregressive covariance structure of order one (ARH1) for K_{sat}.

The distribution of conditional residuals was assessed graphically and using normality diagnostics. Model assumptions were evaluated by visual inspection of residual distributions and fitted-versus-residual plots and were found to be adequate for all final models. All analyses were conducted using the GLIMMIX procedure in SAS (SAS Enterprise Guide 8.6, SAS Institute Inc., Cary, NC, USA).

3. Results

Visual examples of X-ray-imaged soil samples are shown in Fig. 1. Visual inspection indicated that CTRL, G and SL samples were compacted, but the original macropore system was preserved through the study period, and the organization of solid phase remained identifiable throughout the experiment. The PMS samples showed contrasting behaviour, and already after the first field incubation period, the original macropore system had transformed to a new form and the original pores visible in the initial imaging could not be recognized anymore.

The quantitative image analysis led to similar observations. The total visible porosity determined from X-ray tomography images was significantly influenced by imaging round ($p = 0.007$) and imaging round × treatment had a significant interaction effect ($p = 0.012$) (Fig. 2). In the imaging round 0, no differences between treatments were detected, but in the following round, after the first field incubation period, PMS

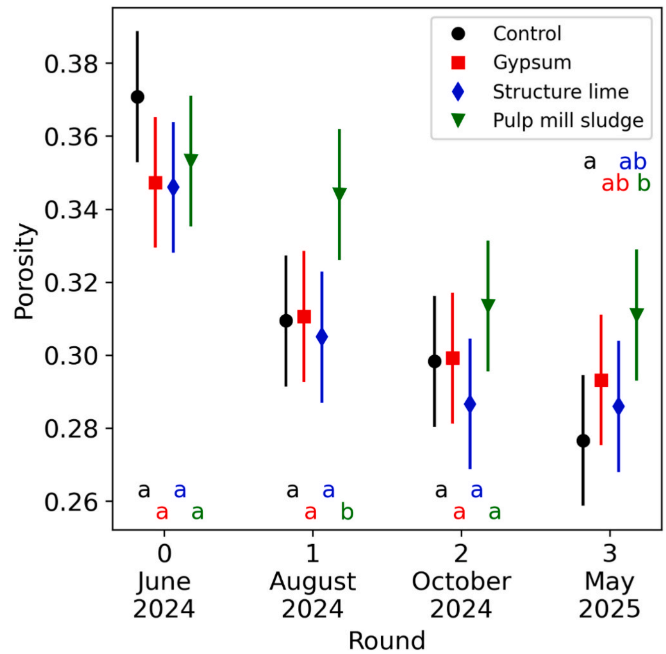

Fig. 2. Total porosity visible in X-ray tomography images and their 95 % confidence intervals for each treatment and imaging round. Significant differences ($p < 0.05$) between treatments for each imaging round are denoted by different letters.

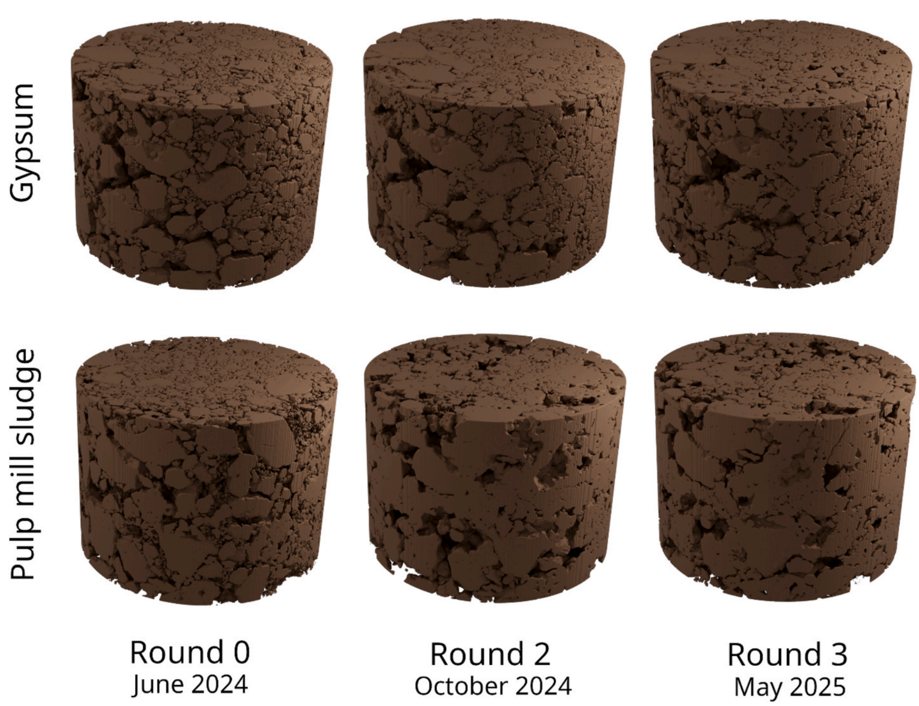

Fig. 1. Visualizations of two sample types (gypsum and pulp mill sludge) at different imaging rounds. Round 0 is the structure before field incubations (June 18, 2024), round 2 in the autumn (October 2–3, 2024) and round 3 after the winter (May 13–14, 2025). Control and structure lime samples behaved similarly to gypsum, i.e., the organization of soil particles and original macropore system could be identified in all imaging rounds.

significantly differed from all other treatments. No statistically significant differences between treatments were detected in the following round, whereas after the winter in the final imaging, PMS significantly differed from CTRL. The porosity in all treatments reduced significantly over the experimental period.

Both imaging round ($p = 0.0097$) and treatment ($p < 0.001$) had significant effects on the pore size distribution (Fig. 3), as indicated by differences among pore size classes. Regarding the temporal dynamics of gypsum and structure lime-treated soils as well as control soil, the smaller-sized macroporosity (<600 μm) decreased during the study period from the initial structural status. For these three treatments, the porosity in the size range of 600–1200 μm decreased during the imaging rounds 0–2, but after the winter, the porosity had increased to the initial level (round 3). The large macroporosity (>1200 μm) remained on the same level in all imaging rounds. PMS-treated soil showed contrasting behaviour in comparison to the three other treatments. The smaller-sized macroporosity (<600 μm) of PMS soil decreased over time, whereas the porosity in the size range of 600–1200 μm remained constant during the study period. However, large macroporosity (>1200 μm) of PMS-treated soil notably increased during the experiment, and the porosity was in the 1200–2000 μm size class more than doubled and in the > 2000 μm size class more than tripled from the initial level (see the Supplementary materials for data and results of statistical comparisons related to differences between imaging rounds).

Regarding the comparisons between treatments, the initial pore size distributions were similar in all treatments (with one exception, see Fig. 3). All significant differences in pairwise comparison between treatments were between PMS-treated soil and the other three treatments (G, SL, CTRL). In contrast, G and SL did not significantly differ from CTRL in any imaging round or pore size class. The contrast between PMS and other treatments was particularly clear for large macroporosity (size classes 1200–2000 μm and > 2000 μm), where the final porosities (round 3) were 2–3 times larger than in the control. In the smaller macropores (classes < 150 μm and 150–300 μm), porosities were, in turn, considerably smaller in PMS than in other treatments in the autumn (round 2). This difference had vanished during the winter, and no differences were detected in the final imaging.

The saturated hydraulic conductivities determined with pore-scale flow simulations showed no significant differences between treatments or imaging round due to large variance in the results (Fig. 4). Nevertheless, PMS showed contrasting behaviour in comparison to other treatments, but none of these differences were statistically significant.

4. Discussion

The structural analyses performed for field-incubated samples showed that soil amendments may influence the development and evolution of the soil macropore system. The results also showed how different amendment types led to contrasting structural effects. The organic PMS amendment had significantly different structural impacts than inorganic G and SL, which, in turn, did not notably differ from each other or from CTRL. Generally, while the samples consolidated during

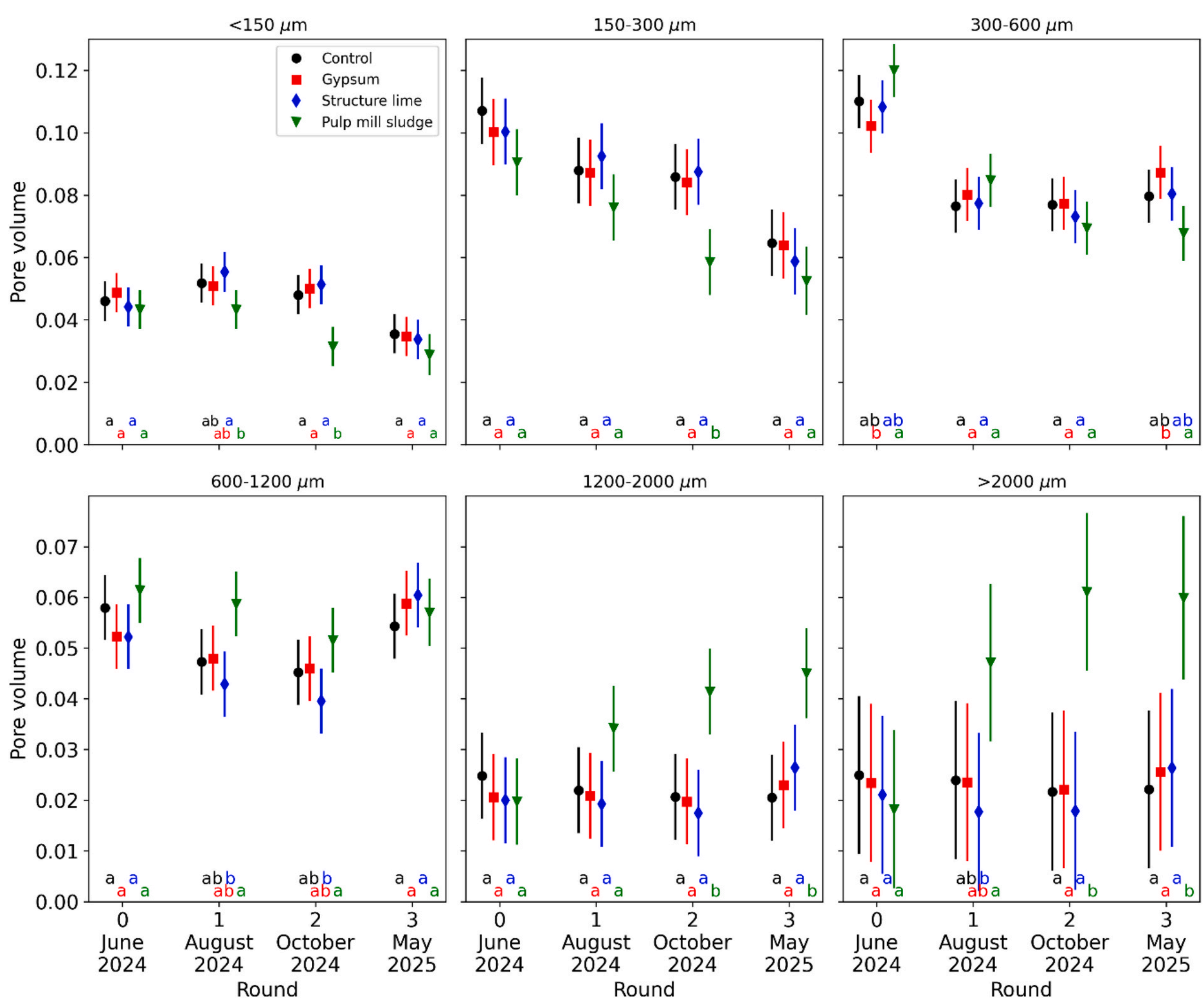

Fig. 3. Porosities of different pore size classes and their 95 % confidence intervals for each treatment and imaging round. Significant differences ($p < 0.05$) between treatments within same pore-size range and imaging round are denoted by different letters.

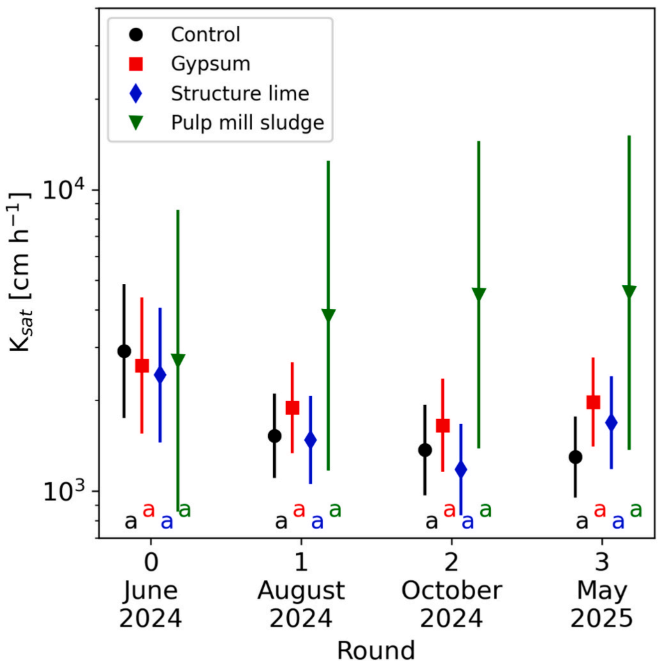

Fig. 4. Saturated hydraulic conductivities (K_{sat}) determined from X-ray tomography images and their 95 % confidence intervals for each treatment and imaging round. Significant differences ($p < 0.05$) between treatments for each imaging round are denoted by different letters.

the field incubation, CTRL, G and SL preserved their original pore structure, and the same pores that were present in the initially packed samples could be identified from the images after the one-year field incubation. PMS addition, in turn, led to the transformation of the soil architecture to a new form already during the first two-month-long field-incubation period. Particularly, PMS increased the share of large macropores. Previously, native organic matter has been reported to have a similar positive impact on macroporosity for Finnish clay soils (Soinne et al. 2023). While PMS led to an increase in large macroporosity, the opposite was detected for smaller macroporosity. Our pore-scale flow simulations did not show statistically significant differences between PMS and other treatments due to the large variance, but the qualitative behaviour of PMS was notably different in comparison to other treatments also in these simulations, indicating the potential of soil amendments to modify the functioning of soil. Unfortunately, the initial macropore structures of PMS samples led to considerably greater variance in simulated hydraulic conductivity as compared to other treatments, which partly explains the lack of statistical significance in the simulation results.

The initial visible porosities of our samples were high compared to previously imaged (with comparable imaging resolution) clay soil samples from Finnish fields (Hyväluoma et al. 2024, 2025; Salminen et al. 2025; Soinne et al. 2023). This was expected as our samples were packed to a reasonably low bulk density to represent topsoil after seedbed preparation, whereas the previous studies have used intact soil samples taken from tilled fields in autumn after the soil had settled during the growing season or from grasslands or no-till fields. Our samples also consolidated during the experimental period but did not reach the values observed in the previous studies. Therefore, it is not surprising that also simulated saturated hydraulic conductivities were on the upper end of the range from previous corresponding simulations (Hyväluoma et al. 2024; Soinne et al. 2023).

The supposed impact mechanism of G and SL on soil structure is similar, as they reduce clay colloid mobilization and induce flocculation of clay colloids by increasing the ionic strength of the soil solution (Uusitalo et al. 2012; Soinne et al. 2025). PMS influences soil structure in a differing mechanism by introducing additional organic matter into soil and enhancing the microbial activity, which further contributes to formation of organo-mineral compounds that bind the soil particles efficiently together (Rasa et al. 2021). Indeed, in soil and environmental conditions comparable to our study, PMS amendment has been reported to increase the microbial-bound C and N pools in soil and change the fungal and bacterial community composition (Rasa et al. 2021), increasing such fungi that have been found to efficiently promote soil aggregation (Lehmann et al. 2020). In contrast, SL-treatment appears to only slightly alter the soil microbial communities (Soinne et al. 2025). Thus, the impact of PMS on soil biological properties is a plausible explanation for the observed contrasts in the structural responses of the studied amendments. These mechanisms appear to alter soil macropore structure more efficiently as compared to impact mechanisms of the studied inorganic amendments. However, it is important to note that since large fauna did not have access to the samples during field-incubation, the formed macroporosity did not result from, e.g., burrowing activity of earthworms. A simple explanation for the increasing volume of large macroporosity in PMS-treated samples would be mineralization of PMS, but the observed remarkable increases of the pore volumes in the two largest pore size classes were considerably greater than the small volume of the added material. Such a simple explanation would also not explain the more comprehensive change that was visually observed. The decrease in the smaller-sized macroporosity (<300 μm) simultaneously with an increase in larger-sized porosity shows that the structure forming processes had opposite impacts in different pore size classes.

The present study did not support the common assumption of positive impacts of G and SL on soil pore structure. In previous studies, gypsum has been found to improve the aggregated stability and to reduce the colloidal detachment (Cox et al. 2005; King et al. 2016; Uusitalo et al. 2012), which nevertheless does not directly indicate changes in soil pore structure. Regarding the structural impacts, some studies have reported changes in partition of runoff components such that gypsum application promotes infiltration and decreases surface runoff (Truman et al. 2010; King et al. 2016; Panday et al., 2019). These results indirectly suggest that in certain conditions G could influence soil macroporosity. However, there are contrasting studies that found no effect of gypsum on the soil hydraulic conductivity (Buckley and Wolkowski 2014), and the observed impacts on infiltration may stem from reduced soil surface sealing due to gypsum's ability to limit clay dispersion (Truman et al. 2010). In our experiment, gypsum had no impact on the hydraulic conductivity in the samples residing below the soil surface, and the results do not indicate changes in the soil pore structure at the spatial scales considered.

The effects of agricultural liming on soil physical properties are also partly conflicting. If the doses of SL used do not raise the pH to the high levels required for pozzolanic cementation reactions (pH≈12.4; Al-Mukhtar et al. 2010), which is a valid assumption for arable soil (Blomquist 2021; Soinne et al. 2025), the soil conditioning effect of SL results largely from similar mechanisms to gypsum. However, relatively small increases in soil pH may stimulate microbiological activity and increase soil productivity (Pietri & Brookes, 2008). As both processes contribute to soil structural stability (Bronick & Lal, 2005; Costa et al. 2018), this suggests that SL may also indirectly enhance aggregate stability via biologically mediated pathways. SL has been found to promote the soil structural stability in several studies (Soinne et al. 2025; Blomquist et al. 2018, 2022b; Keiblinger et al. 2016). Liming with agricultural lime ($CaCO_3$) has been reported to affect also other structural properties than stability (Holland et al. 2018). Frank et al. (2019, 2020) found that liming significantly affected several soil physical parameters (bulk density, total porosity, plant available water, hydraulic conductivity) six months after liming, but the effects seemed to vanish after tillage and liming did not induce a long-term change in the soil structure. Regarding SL, Zimmermann et al. (2016) found that the addition of quicklime resulted in higher air capacity, air permeability and saturated hydraulic conductivity. Concerning the soil pore structure, there are contrasting results as there are studies reporting increasing (Carmeis Filho et al. 2016) and decreasing (Bölscher et al. 2021) macroporosity. These controversial results suggest that in some conditions SL may have a more noticeable impact on soil structure than in the present study, even though in our study conditions the effect turned out to be insignificant.

Previous studies support our finding on the positive impact of PMS on soil macroporosity. On coarse-textured soil, PMS has been reported to increase saturated hydraulic conductivity (Chow et al. 2003; Räty et al. 2024), which is sensitive to large macropores. Räty et al. (2024) also reported a decline in readily plant-available water. While our study did not cover the pore size region matching with the readily plant available water (i.e. 1–30 μm), we found a decrease in small macroporosity, which suggests that PMS can have opposite effects on different pore size regions similarly to the findings of Räty et al. (2024) for a differing soil type. Rasa et al. (2024) studied structural properties in PMS-amended clay soil comparable to that considered in the present study and found an increase in large microporosity (> 80 μm), which again agrees with our findings. The type and quality of organic material may also influence the structure evolution induced by the amendment. In our study, PMS was lime stabilized but if hygienization was instead done by composting, which is one viable option, the resulting organic product would decompose more slowly in the soil, which might affect its structural impacts.

The changes in macropore systems induced especially by PMS treatment can have consequences for soil physical processes and functions. The increase in soil macroporosity is essential for, e.g., hydraulic conductivity and air permeability of soil (Heard et al. 1988). Increased hydraulic conductivity of soil promotes flow through subsurface drainage and reduces the risk of surface runoff-induced soil and nutrient losses during intense rains (Gupta et al. 2024). On the other hand, large macroporosity can generate preferential flow in larger macropores, thus promoting rapid transport of nutrients and other agrochemicals to subsurface drainage (Jarvis 2007). However, flow occurring through a dense and homogeneously distributed macropore network may prevent fast preferential transport as compared to a macropore network dominated by a few large macropores bypassing the soil matrix (Larsbo et al. 2016).

The present work was the first study utilizing time-lapse imaging of field-incubated soil samples to investigate the structural dynamics of soil treated with soil amendments. The study was limited to one soil and three amendments with a single dose for each material. Previous studies have shown that the effect of soil amendments can be site (Bölscher et al. 2021) and dose (Blomquist et al. 2018) specific. Thus, the results obtained here cannot be directly generalized to differing soil and climatic conditions or to other amendment types. However, the results show beyond doubt that the used approach can observe the influences of various types of soil amendments on soil structure dynamics and distinguish the differences between the amendment type.

The used method enables tracking of structural changes of the samples exposed to the real environmental conditions. However, there are obvious limitations to fully realistic field conditions, most importantly the absence of plants in the samples due to the limited sample size. We characterized the macropore structure with easily comprehensible parameters such as porosity and pore-size distribution. It is noteworthy that more complicated metrics with higher information content exist, which provide a more comprehensive but less comprehensible quantification of soil structure dynamics (Tolstygin et al. 2026).

Soil structure studies based on X-ray tomography unavoidably lead to balancing between the sample size and image resolution, even though stitching approaches provide means to alleviate this limitation (Englisch et al. 2023; Miettinen et al. 2019). In the present study, the centimetre-scale sample size was selected to comply with those typically used in soil imaging studies and water retention measurements, which limited the focus of this study to macroporosity. Aggregate-level imaging of amended soil has been performed in a few earlier studies (e.g. Bölscher et al. 2021; Heikkinen et al. 2019; Rasa et al. 2024). Imaging of millimetre-sized aggregates allows order-of-magnitude improvement in the resolution, but the sample size used may not be reasonable in field-incubation studies. An even larger sample size than that used in the present work would be necessary to investigate the effects of plants and plant roots on soil structure dynamics, as the repeated excavation of the samples disturbs the roots passing between the sample and the surrounding soil. Regarding the pore-scale flow simulations, the approach has been shown to be a robust method for estimating saturated hydraulic conductivity if sufficient imaging resolution is able to distinguish the main connected porosity, although exact agreement with experiments cannot be expected (Gerke et al. 2026). In addition to imaging resolution, uncertainties in segmentation (Gerke et al. 2026) and limited sample height (Soinne et al. 2023) affect the accuracy of the approach. In the current study, the soil structure of samples remained undisturbed during the study period. Tillage is known to affect the structure (Schlüter et al. 2018), and as noted earlier, it is possible that the structural impacts of soil amendments may vanish after tillage events (Frank et al. 2019).

5. Conclusions

This research investigated the structural effects of three soil amendments using X-ray tomography and time-lapse imaging of clay soil samples field-incubated in a boreal climate for a one-year period. Our results showed that amendments can notably affect the soil macroporosity, but the impact was dependent on the type of amendment. The two inorganic amendments considered, gypsum and structure lime, did not notably influence the soil macroporosity. The organic pulp mill sludge, in turn, clearly affected the macropore system by increasing the volume of macroporosity in the millimetre size range. The opposite was observed for smaller macropores (<300 μm) after the samples were exposed to field conditions, but the differences in this pore size class vanished during the winter period. The results show that, in addition to its use as a water protection measure through soil structure stabilization, pulp mill sludge can also alter the macropore system, thereby influencing other soil functions mediated by soil macroporosity. The doses of all amendments corresponded to the common application rates in field use, whereby we expect the observations to be useful for practical applications. The extent to which the results generalize to other soil types and environmental conditions requires further investigation. However, as the impacts occurred in short temporal scales and did not require, e.g., a cold winter with freezing-thawing cycles, we expect that the results can be generalized outside the study region. Our results also demonstrate that time-lapse imaging of field-incubated soil samples is an efficient tool for studying structural dynamics of soils amended with potential soil-improving materials.

CRediT authorship contribution statement

Jari Hyväluoma: Writing – review & editing, Writing – original draft, Visualization, Methodology, Investigation, Formal analysis, Conceptualization. **Idil Ertem:** Writing – review & editing, Writing – original draft, Investigation, Formal analysis. **Arttu Miettinen:** Writing – review & editing, Resources, Investigation, Conceptualization. **Janne Kaseva:** Writing – review & editing, Writing – original draft, Formal analysis. **Helena Soinne:** Writing – review & editing, Resources, Conceptualization. **Sami Kinnunen:** Investigation. **Tero Harjupatana:** Investigation. **Riikka Keskinen:** Writing – review & editing, Writing – original draft, Conceptualization.

Declaration of competing interest

The authors declare that they have no known competing financial interests or personal relationships that could have appeared to influence the work reported in this paper.

Acknowledgments

This work was funded by The Finnish Research Impact Foundation. This project also received funding from the European Union's Horizon Europe programme under grant agreement No 101181712 (GREEN-HOOD). The results reported in this paper reflect only the authors' views, and the European Commission is not responsible for any use that may be made of the information it contains. CSC–IT Center for Science is acknowledged for computing time through project #2005253.

Appendix A. Supplementary data

Supplementary data to this article can be found online at https://doi.org/10.1016/j.geoderma.2026.117995.

Data availability

The image analysis data that support the findings of this study are available as Supplementary material.

References

Al-Mukhtar, M., Lasledj, A., Alcover, J.F., 2010. Behaviour and mineralogy changes in lime-treated expansive soil at 20°C. Appl. Clay Sci. 50 (2), 191–198. https://doi.org/10.1016/j.clay.2010.07.023.

Barthod, J., Rumpel, C., & Dignac, M. F. (2018). Composting with additives to improve organic amendments. A review. Agronomy for Sustainable Development, 38(2), 17. doi: 10.1007/s13593-018-0491-9.

Arrázola Vásquez, E., 2023. Effects of soil compaction on burrowing and energy costs of different earthworm species. [Swedish University of Agricultural Sciences]. https://doi.org/10.54612/a.5fhh1r6sg4.

Blomquist, J., 2021. Effects of structure liming on clay soil. Doctoral thesis, Swedish University of Agricultural Sciences. Acta Universitatis Agriculturae Sueciae 86.

Blomquist, J., Englund, J.E., Berglund, K., 2022a. Site characteristics determine the duration of structure liming effects on clay soil. Agricultural and Food Science 31 (3), 136–148. https://doi.org/10.23986/afsci.115313.

Blomquist, J., Englund, J.E., Berglund, K., 2022b. Soil characteristics and tillage can predict the effect of "structure lime" on soil aggregate stability. Soil Research 60 (4), 373–384. https://doi.org/10.1071/SR21022.

Blomquist, J., Englund, J.E., Sjöberg, C., Kårhammer, J., Svensson, S.E., Pettersson, E., Keller, T., Berglund, K., 2023. Structure liming reduces draught requirement on clay soil. Soil and Tillage Research 231, 105703. https://doi.org/10.1016/j.still.2023.105703.

Blomquist, J., Simonsson, M., Etana, A., Berglund, K., 2018. Structure liming enhances aggregate stability and gives varying crop responses on clayey soils. Acta Agriculturae Scandinavica Section b: Soil and Plant Science 68 (4), 311–322. https://doi.org/10.1080/09064710.2017.1400096.

Bronick, C.J., Lal, R., 2005. Soil structure and management: a review. Geoderma 124 (1–2), 3–22. https://doi.org/10.1016/j.geoderma.2004.03.005.

Buckley, M.E., Wolkowski, R.P., 2014. In-season effect of Flue Gas Desulfurization Gypsum on Soil Physical Properties. Journal of Environmental Quality 43 (1), 322–327. https://doi.org/10.2134/jeq2012.0354.

Bölscher, T., Koestel, J., Etana, A., Ulen, B., Berglund, K., Larsbo, M., 2021. Changes in pore networks and readily dispersible soil following structure liming of clay soils. Geoderma 390, 114948. https://doi.org/10.1016/j.geoderma.2021.114948.

Camberato, J.J., Gagnon, B., Angers, D.A., Chantigny, M.H., Pan, W.L., 2006. Pulp and paper mill by-products as soil amendments and plant nutrient sources. Canadian Journal of Soil Science 86, 641–653.

Carmeis Filho, A.C.A., Crusciol, C.A.C., Guimarães, T.M., Calonego, J.C., Mooney, S.J., 2016. Impact of amendments on the physical properties of soil under tropical long-term no till conditions. PLoS ONE 11 (12), e0167564. https://doi.org/10.1371/journal.pone.0167564.

Chow, T.L., Rees, H.W., Fahmy, S.H., Monteith, J.O., 2003. Effects of pulp fibre on soil physical properties and soil erosion under simulated rainfall. Canadian Journal of Soil Science 83, 109–119. https://doi.org/10.4141/S02-009.

Costa, O.Y.A., Raaijmakers, J.M., Kuramae, E.E., 2018. Microbial Extracellular Polymeric Substances: Ecological Function and Impact on Soil Aggregation. Frontiers in Microbiology 9, 1636. https://doi.org/10.3389/fmicb.2018.01636.

Cox, J.W., Varcoe, J., Chittleborough, D.J., van Leeuwen, J., 2005. Using Gypsum to Reduce Phosphorus in Runoff from Subcatchments in South Australia. Journal of Environmental Quality 34 (6), 2118–2128. https://doi.org/10.2134/jeq2005.0013.

d'Humières, D., Ginzburg, I., 2009. Viscosity independent numerical errors for Lattice Boltzmann models: from recurrence equations to "magic" collision numbers. Computers and Mathematics with Applications 58 (5), 823–840. https://doi.org/10.1016/j.camwa.2009.02.008.

Ekholm, P., Ollikainen, M., Punttila, E., Ala-Harja, V., Riihimäki, J., Kiirikki, M., Taskinen, A., Begum, K., 2024. Gypsum amendment of agricultural fields to decrease phosphorus losses – evidence on a catchment scale. Journal of Environmental Management 357. https://doi.org/10.1016/j.jenvman.2024.120706.

Englisch, S., Wirth, J., Drobek, D., Apeleo Zubiri, B., Spiecker, E., 2023. Expanding accessible 3D sample size in lab-based X-ray nanotomography without compromising resolution. Precision Engineering 82, 169–183. https://doi.org/10.1016/j.precisioneng.2023.02.011.

Feldkamp, L.A., Davis, L.C., Kress, J.W., 1984. Practical Cone-Beam Algorithm. Journal of the Optical Society of America A 1, 612–619. https://doi.org/10.1364/JOSAA.1.000612.

Foley, B.J., Cooperband, L.R., 2002. Paper Mill Residuals and Compost Effects on Soil Carbon and Physical Properties. Journal of Environmental Quality 31 (6), 2086–2095. https://doi.org/10.2134/jeq2002.2086.

Frank, T., Zimmermann, I., Horn, R., 2019. The need for lime in dependence on clay content in arable crop production in Germany. Soil and Tillage Research 191, 11–17. https://doi.org/10.1016/j.still.2019.03.013.

Frank, T., Zimmermann, I., Horn, R., 2020. Lime application in marshlands of Northern Germany—Influence of liming on the physicochemical and hydraulic properties of clayey soils. Soil and Tillage Research 204, 104730. https://doi.org/10.1016/j.still.2020.104730.

Garbowski, T., Bar-Michalczyk, D., Charazińska, S., Grabowska-Polanowska, B., Kowalczyk, A., Lochyński, P., 2023. An overview of natural soil amendments in agriculture. Soil and Tillage Research 225, 105462. https://doi.org/10.1016/j.still.2022.105462.

Gerke, K. M., Khirevich, S., Vasilyev, R. v., Karsanina, M. v., Umarova, A. B., Barbosa, L. A. P., Korost, D. v., Tolstygin, K. D., Mallants, D., & Gerke, H. H. (2026). Soil hydraulic properties derived from pore-scale simulations: Digital assessment of K_{sat} through model intercomparison and verification with experimental data. Soil and Tillage Research, 255, 106790. doi: 10.1016/j.still.2025.106790.

Ginzburg, I., Verhaeghe, F., dHumìeres, D., 2008. Two-Relaxation-Time Lattice Boltzmann Scheme: about Parametrization, Velocity, pressure and mixed Boundary Conditions. Communications in Computational Physics 3 (2), 427–478. http://www.global-sci.com/427.

Gonzalez, R.C., Woods, R.E., 2008. Digital Image Processing, 3rd ed. Pearson Education International.

Grieve, I.C., Davidson, D.A., Bruneau, P.M.C., 2005. Effects of liming on void space and aggregation in an upland grassland soil. Geoderma 125 (1–2), 39–48. https://doi.org/10.1016/j.geoderma.2004.06.004.

Gupta, S., Borrelli, P., Panagos, P., Alewell, C., 2024. An advanced global soil erodibility (K) assessment including the effects of saturated hydraulic conductivity. Science of the Total Environment 908, 168249. https://doi.org/10.1016/j.scitotenv.2023.168249.

Heard, J.R., Kladivko, E.J., Mannering, J.V., 1988. Soil Macroporosity, Hydraulic Conductivity and Air Permeability of Silty Soils under Long-Term Conservation Tillage in Indiana. Soil & Tillage Research 11, 1–18. https://doi.org/10.1016/0167-1987(88)90027-X.

Heikkinen, J., Keskinen, R., Soinne, H., Hyväluoma, J., Nikama, J., Wikberg, H., Källi, A., Siipola, V., Melkior, T., Dupont, C., Campargue, M., Larsson, S.H., Hannula, M., Rasa, K., 2019. Possibilities to improve soil aggregate stability using biochars derived from various biomasses through slow pyrolysis, hydrothermal carbonization, or torrefaction. Geoderma 344, 40–49. https://doi.org/10.1016/j.geoderma.2019.02.028.

Heikkinen, J., Ketoja, E., Seppänen, L., Luostarinen, S., Fritze, H., Pennanen, T., Peltoniemi, K., Velmala, S., Hanajik, P., Regina, K., 2021. Chemical composition controls the decomposition of organic amendments and influences the microbial community structure in agricultural soils. Carbon Management 12 (4), 359–376. https://doi.org/10.1080/17583004.2021.1947386.

Hellner, Q., Koestel, J., Ulén, B., Larsbo, M., 2018. Effects of tillage and liming on macropore networks derived from X-ray tomography images of a silty clay soil. Soil Use and Management 34 (2), 197–205. https://doi.org/10.1111/sum.12418.

Holland, J.E., Bennett, A.E., Newton, A.C., White, P.J., McKenzie, B.M., George, T.S., Pakeman, R.J., Bailey, J.S., Fornara, D.A., Hayes, R.C., 2018. Liming impacts on soils, crops and biodiversity in the UK: a review. Science of the Total Environment 610–611, 316–332. https://doi.org/10.1016/j.scitotenv.2017.08.020.

Horgan, G.W., 1998. Mathematical morphology for analysing soil structure from images. European Journal of Soil Science 49, 161–173. https://doi.org/10.1046/j.1365-2389.1998.00160.x.

Hyväluoma, J., Niemi, P., Kinnunen, S., Brobbey, K., Miettinen, A., Keskinen, R., Soinne, H., 2024. Comparing structural soil properties of boreal clay fields under contrasting soil management. Soil Use and Management 40 (2), e13040. https://doi.org/10.1111/sum.13040.

Hyväluoma, J., Niemi, V., Thapaliya, M., Turtola, E., Järnstedt, J., Timonen, J., 2018. Lattice Boltzmann simulation of Flow-Induced Wall Shear stress in Porous Media. Transport in Porous Media 121, 353–368. https://doi.org/10.1007/s11242-017-0967-0.

Iho, A., Laukkanen, M., 2012. Gypsum amendment as a means to reduce agricultural phosphorus loading: an economic appraisal. Agricultural and Food Science 21, 307–324. https://doi.org/10.23986/afsci.6832.

Jarvis, N.J., 2007. A review of non-equilibrium water flow and solute transport in soil macropores: principles, controlling factors and consequences for water quality. European Journal of Soil Science 58 (3), 523–546. https://doi.org/10.1111/j.1365-2389.2007.00915.x.

Keiblinger, K.M., Bauer, L.M., Deltedesco, E., Holawe, F., Unterfrauner, H., Zehetner, F., Peticzka, R., 2016. Quicklime application instantly increases soil aggregate stability. International Agrophysics 30 (1), 123–128. https://doi.org/10.1515/intag-2015-0068.

Keskinen, R., Soinne, H., Uusitalo, R., Ekholm, P., Räsänen, T.A., Uusi-Kämppä, J., Bergholm, J., Nikama, J., Hyväluoma, J., 2025. Soil Properties-based Targeting of

Soil Conditioners for Reduced Phosphorus Loading from Agriculture. European Journal of Soil Science 76 (3), e70143. https://doi.org/10.1111/ejss.70143.
Keskinen, R., Suojala-Ahlfors, T., Sarvi, M., Hagner, M., Kaseva, J., Salo, T., Uusitalo, R., 2020. Granulated broiler manure based organic fertilizers as sources of plant available nitrogen. Environmental Technology and Innovation 18, 100734. https://doi.org/10.1016/j.eti.2020.100734.
King, K.W., Williams, M.R., Dick, W.A., LaBarge, G.A., 2016. Decreasing Phosphorus loss in Tile-Drained Landscapes using Flue Gas Desulfurization Gypsum. Journal of Environmental Quality 45 (5), 1722–1730. https://doi.org/10.2134/jeq2016.04.0132.
Koestel, J., Schlüter, S., 2019. Quantification of the structure evolution in a garden soil over the course of two years. Geoderma 338, 597–609. https://doi.org/10.1016/j.geoderma.2018.12.030.
Kost, D., Ladwig, K.J., Chen, L., DeSutter, T.M., Espinoza, L., Norton, L.D., Smeal, D., Torbert, H.A., Watts, D.B., Wolkowski, R.P., Dick, W.A., 2018. Meta-Analysis of Gypsum Effects on Crop yields and Chemistry of Soils, Plant Tissues, and Vadose Water at Various Research Sites in the USA. Journal of Environmental Quality 47 (5), 1284–1292. https://doi.org/10.2134/jeq2018.04.0163.
Koszinski, S., Wendroth, O., Lehfeldt, J., 1995. Field scale heterogeneity of soil structural properties in a moraine landscape of north-eastern Germany. International Agrophysics 9, 201–210.
Larney, F.J., Angers, D.A., 2012. The role of organic amendments in soil reclamation: a review. Canadian Journal of Soil Science 92 (1), 19–38. https://doi.org/10.4141/CJSS2010-064.
Larsbo, M., Koestel, J., Kätterer, T., Jarvis, N., 2016. Preferential Transport in Macropores is Reduced by Soil Organic Carbon. Vadose Zone Journal 15 (9). https://doi.org/10.2136/vzj2016.03.0021.
Larsbo, M., Koestel, J., Jarvis, N., 2014. Relations between macropore network characteristics and the degree of preferential solute transport. Hydrology and Earth System Sciences 18 (12), 5255–5269. https://doi.org/10.5194/hess-18-5255-2014.
Lehmann, A., Zheng, W., Ryo, M., Soutschek, K., Roy, J., Rongstock, R., Maaß, S., Rillig, M.C., 2020. Fungal Traits Important for Soil Aggregation. Frontiers in Microbiology 10, 2904. https://doi.org/10.3389/fmicb.2019.02904.
Leuther, F., Mikutta, R., Wolff, M., Kaiser, K., Schlüter, S., 2023. Structure turnover times of grassland soils under different moisture regimes. Geoderma 433. https://doi.org/10.1016/j.geoderma.2023.116464.
Lilja, H., Uusitalo, R., Yli-Halla, M., Nevalainen, R., Väänänen, T., Tamminen, P., Tuhtar, J. (2017). Suomen maannostietokanta: Käyttöopas versio 1.1 - Geographical soil database of Finland: Users' manual version 1.1. Luonnonvara- ja biotalouden tutkimus 6/2017. http://urn.fi/URN:ISBN:978-952-326-357-4.
Liu, H., Kang, Q., Leonardi, C.R., Schmieschek, S., Narváez, A., Jones, B.D., Williams, J. R., Valocchi, A.J., Harting, J., 2016. Multiphase lattice Boltzmann simulations for porous media applications: a review. Computational Geosciences 20 (4), 777–805. https://doi.org/10.1007/s10596-015-9542-3.
Miettinen, A., Oikonomidis, I.V., Bonnin, A., Stampanoni, M., 2019. NRStitcher: Non-rigid stitching of terapixel-scale volumetric images. Bioinformatics 35 (24), 5290–5297. https://doi.org/10.1093/bioinformatics/btz423.
O'Connor, J., Mickan, B.S., Rinklebe, J., Song, H., Siddique, K.H.M., Wang, H., Kirkham, M.B., Bolan, N.S., 2022. Environmental implications, potential value, and future of food-waste anaerobic digestate management: a review. Journal of Environmental Management 318, 115519. https://doi.org/10.1016/j.jenvman.2022.115519.
Ollikainen, M., Lötjönen, S., Tikkanen, T., Ala-Harja, V., Uusitalo, R., Ekholm, P., 2024. Gypsum and structure lime amendments in boreal agricultural clay soils: do climate emissions compromise water quality benefits? Agricultural and Food Science 33 (2), 90–115. https://doi.org/10.23986/afsci.143577.
Panday, D., Ferguson, R., & Maharjan, B. (2019). Flue Gas Desulfurization Gypsum as Soil Amendment. In Soil Amendments for Sustainability: Challenges and Perspectives, eds. Rakshit, A., Sarkar, B., & Abhilash, P.C. (Boca Raton, Taylor & Francis Group, LLC).
Pietri, J.A., Brookes, P.C., 2008. Relationships between soil pH and microbial properties in a UK arable soil. Soil Biology and Biochemistry 40 (7), 1856–1861. https://doi.org/10.1016/j.soilbio.2008.03.020.
Poeplau, C., Prietz, R., Don, A., 2022. Plot-scale variability of organic carbon in temperate agricultural soils—Implications for soil monitoring. Journal of Plant Nutrition and Soil Science 185 (3), 403–416. https://doi.org/10.1002/jpln.202100393.
Rasa, K., Pennanen, T., Peltoniemi, K., Velmala, S., Fritze, H., Kaseva, J., Joona, J., Uusitalo, R., 2021. Pulp and paper mill sludges decrease soil erodibility. Journal of Environmental Quality 50 (1), 172–184. https://doi.org/10.1002/jeq2.20170.
Rasa, K., Tähtikarhu, M., Miettinen, A., Kähärä, T., Uusitalo, R., Mikkola, J., Hyväluoma, J., 2024. A large one-time addition of organic soil amendments increased soil macroporosity but did not affect intra-aggregate porosity of a clay soil. Soil and Tillage Research 242, 106139. https://doi.org/10.1016/j.still.2024.106139.
Räty, M., Termonen, M., Hyvönen, J., Uusi-Kämppä, J., Järvenranta, K., Soinne, H., Nikama, J., Rasa, K., Järvinen, M., Keskinen, R., 2024. The amendment value of pulp and paper mill sludges in finnish coarse-textured soil. Geoderma Regional 39. https://doi.org/10.1016/j.geodrs.2024.e00894.
Salminen, J., Hyväluoma, J., Adamczyk, B., Adamczyk, S., Niemi, P., Kinnunen, S., Miettinen, A., 2025. Trophic interactions and microbial-derived carbon in porosphere of arable fields. Soil Biology and Biochemistry 210, 109924. https://doi.org/10.1016/j.soilbio.2025.109924.
Schlüter, S., Albrecht, L., Schwärzel, K., Kreiselmeier, J., 2020. Long-term effects of conventional tillage and no-tillage on saturated and near-saturated hydraulic conductivity – can their prediction be improved by pore metrics obtained with X-ray CT? Geoderma 361, 114082. https://doi.org/10.1016/j.geoderma.2019.114082.
Schlüter, S., Großmann, C., Diel, J., Wu, G.M., Tischer, S., Deubel, A., Rücknagel, J., 2018. Long-term effects of conventional and reduced tillage on soil structure, soil ecological and soil hydraulic properties. Geoderma 332, 10–19. https://doi.org/10.1016/j.geoderma.2018.07.001.
Soinne, H., Fritze, H., Pennanen, T., Velmala, S., Räty, M., Uusitalo, R., 2025. Structure Lime as a Soil Amendment: Impacts on Nutrient loss risk and Soil Health. European Journal of Soil Science 76 (5), e70193. https://doi.org/10.1111/ejss.70193.
Soinne, H., Keskinen, R., Tähtikarhu, M., Kuva, J., Hyväluoma, J., 2023. Effects of organic carbon and clay contents on structure-related properties of arable soils with high clay content. European Journal of Soil Science 74 (5), e13424. https://doi.org/10.1111/ejss.13424.
Tahir, S., Marschner, P., 2016. Clay amendment to sandy soil—effect of clay concentration and ped size on nutrient dynamics after residue addition. Journal of Soils and Sediments 16 (8), 2072–2080. https://doi.org/10.1007/s11368-016-1406-5.
Tan, E.H., Zahran, E.M.M., Tan, S.J., 2020. A review of chemical stabilisation in road construction. IOP Conference Series: Materials Science and Engineering 943 (1), 012005. https://doi.org/10.1088/1757-899X/943/1/012005.
Tolstygin, K. D., Zubov, A. S., Karsanina, M. v., Kulygin, D. A., Fomin, D. S., Yudina, A. v., Romanenko, K. A., & Gerke, K. M. (2026). Morphological and topological dynamics of soil pore structure during wetting–drying. Soil and Tillage Research, 256, 106895. doi: 10.1016/j.still.2025.106895.
Truman, C.C., Nuti, R.C., Truman, L.R., Dean, J.D., 2010. Feasibility of using FGD gypsum to conserve water and reduce erosion from an agricultural soil in Georgia. Catena 81 (3), 234–239. https://doi.org/10.1016/j.catena.2010.04.003.
Turunen, M., Hyväluoma, J., Heikkinen, J., Keskinen, R., Kaseva, J., Koestel, J., Rasa, K., 2019. Quantifying Physical Properties of three Sphagnum-based growing Media as Affected by Drying – Wetting Cycles. Vadose Zone Journal 18, 190033. https://doi.org/10.2136/vzj2019.04.0033'.
Ulén, B., Etana, A., 2014. Phosphorus leaching from clay soils can be counteracted by structure liming. Acta Agriculturae Scandinavica Section b: Soil and Plant Science 64 (5), 425–433. https://doi.org/10.1080/09064710.2014.920043.
Uusitalo, R., Ylivainio, K., Hyväluoma, J., Rasa, K., Kaseva, J., Nylund, P., Pietola, L., Turtola, E., 2012. The effects of gypsum on the transfer of phosphorus and other nutrients through clay soil monoliths. Agricultural and Food Science 21, 260–278. https://doi.org/10.23986/afsci.4855.
Zimmermann, I., Fleige, H., Horn, R., 2016. Soil structure amelioration with quicklime and irrigation experiments in earth graves. Journal of Soils and Sediments 16 (11), 2514–2522. https://doi.org/10.1007/s11368-016-1509-z.